Geophysical Research Letters®

Correspondence to:

J. C. L. Chan and R. Ding,
Johnny.chan@cityu.edu.hk;
drq@bnu.edu.cn

Author Contributions:

Conceptualization: Quanjia Zhong
Investigation: Quanjia Zhong
Methodology: Quanjia Zhong
Supervision: Wansuo Duan, Johnny C. L. Chan, Ruiqiang Ding
Writing – original draft: Quanjia Zhong
Writing – review & editing: Quanjia Zhong, Wansuo Duan, Shifei Tu, Yongjie Huang, Johnny C. L. Chan, Ruiqiang Ding

Landward Acceleration of Tropical Cyclones Making Landfall Along the South China Coast

Quanjia Zhong[1] , Wansuo Duan[2] , Shifei Tu[3] , Yongjie Huang[4] , Johnny C. L. Chan[5,6,7] , and Ruiqiang Ding[8]

[1]Department of Ocean Science, Center for Ocean Research in Hong Kong and Macau (CORE) Hong Kong University of Science and Technology, Hong Kong, China, [2]State Key Laboratory of Earth System Numerical Modeling and Application, Institute of Atmospheric Physics, Chinese Academy of Sciences, Beijing, China, [3]South China Sea Institute of Marine Meteorology/Western Guangdong Key Laboratory of Marine Meteorological Disaster Theory and Application, College of Ocean and Meteorology, Guangdong Ocean University, Zhanjiang, China, [4]Center for Analysis and Prediction of Storms, University of Oklahoma, Norman, Oklahoma, USA, [5]School of Energy and Environment, City University of Hong Kong, Hong Kong, China, [6]Asia-Pacific Typhoon Collaborative Research Center, Shanghai, China, [7]Shanghai Typhoon Institute, China Meteorological Administration, Shanghai, China, [8]State Key Laboratory of Earth Surface Processes and Disaster Risk Reduction, Beijing Normal University, Beijing, China

Abstract Accurate forecasts of near-landfall TC characteristics (direction, translation speed, and intensity) are essential for timely disaster preparedness. Using best-track data (1951–2023), this study reveals a significant pre-landfall acceleration of TCs along the South China coast, with translation speed increasing by 35.5% and 16.4% during the 24 hr prior to landfall for eastbound and westbound cases, respectively. This acceleration is primarily contributed by the normal component of the translation vector. For westbound TCs, translation speed and its normal component increase with intensity, particularly at typhoon strength and above. Numerical simulations and diagnostic analyses attribute the acceleration to horizontal advection and diabatic heating, primarily driven by land-induced asymmetric flow and convection. These findings strengthen the current understanding of TC motion dynamics and support more effective disaster prevention and mitigation strategies as TCs approach coastal regions.

Plain Language Summary Changes in the translation speed of tropical cyclones (TCs) pose great challenges in disaster preparedness. Specifically, the normal and parallel components of TC translation vectors relative to coastal orientation are strongly associated with landfall time and location, respectively. However, little is known about the processes that could lead to short-term changes in each of these two components. This study finds that landfalling TCs tend to accelerate as they approach the South China coast, with the main contribution to this acceleration coming from the component of the TC motion normal to the coastline. The acceleration is primarily driven by land-induced asymmetric flow and convection. Understanding the mechanism responsible for these changes in the two components of the TC translation speed is critical for predicting landfall time and location, thereby improving disaster preparedness in the region.

1. Introduction

Tropical cyclones (TCs) that approach the coast pose a great threat to life and property. A good prediction of the evolution of TC characteristics, such as intensity, motion direction, translation speed, and rainfall distribution, would help to reduce the loss of life and minimize the damage. Particularly, the translation speed is one of the most important characteristics of TC due to the fact that the local TC rainfall usually increases with rain rate near the center and decreases with translation speed (Emanuel, 2017; Risser & Wehner, 2017).

TC translation speed has received much attention after a global slowdown with global warming was reported by Kossin (2018). He also suggested that slowdown of TCs would ultimately result in the increase of local rainfall in a warming climate. However, such finding and implication are still arguable due to the inhomogeneity of the observed best-track data from the pre-satellite to the post-satellite era (Chan, 2019; Lanzante, 2019; Moon et al., 2019). Yamaguchi et al. (2020) further showed that global TCs did not move slowdown in the past, and their mean translation speed could increase with global warming but would decrease as TCs move into the extratropic. Moreover, some studies also revealed the interannual and multidecadal variability of translation speed of TCs over the western North Pacific and the South of China Sea and most of them attributes these to the large-scale

steering flow and the variations of sea surface temperature (Guo et al., 2023; Shan et al., 2023; Wang et al., 2020; Wu et al., 2022). Although these studies have greatly enhanced our comprehension of TC translation speed and its attributions, they primarily concentrate on the long-term changes, interannual and interdecadal variations of TC translation speed across the entire ocean basin. On the other hand, the understanding of short-term (i.e., hour-to-day timescales) changes in translation speed during TCs landfall, which is crucial for effective disaster preparedness efforts especially in highly-populated coastal areas (e.g., the South China coast), is still relatively limited.

Our previous study revealed that TCs globally tend to accelerate as they approach the coast, with land effects potentially being one of the dominant driving factors (Zhong et al., 2025). Although a universal acceleration characteristic of landfalling TCs has been identified, the influence of coastline orientation on TC motion remains unclear, given the substantial differences in coastline orientation across regions and basins globally. For example, the coastlines of Japan and the eastern coastline of North America are primarily oriented southwest to northeast, those of eastern China and Vietnam are oriented north to south, and the eastern North Pacific coastlines exhibit a southeast to northwest orientation, with the South China coastline also following a southwest to northeast orientation.

In particular, landfalling TCs along the South China coast exhibit behavior that deviates from the globally averaged characteristic, owing to the coexistence of distinct track types and their strong coupling with the coastline orientation (Chan et al., 2004; Huang et al., 2025; Wu et al., 2022). On the one hand, some TCs form locally over the South China Sea and move eastward or westward to make landfall along the South China coast. On the other hand, TCs originating in the western North Pacific often first make landfall over the Philippine archipelago before reentering the South China Sea, where they may reintensify and subsequently make landfall along the South China coast.

As the South China coast experiences the highest number of landfalling TCs along the East Asia coastline, with an annual average of six to seven landfalling events (Sajjad & Chan, 2019), both coastline orientation and regional geographic characteristics strongly influence TC tracks and motion near landfall. Understanding the physical mechanisms governing changes in TC movement near landfall is therefore critical for improving predictions of landfall location and timing. In this study, rather than re-establishing the existence of landward acceleration, we introduce a coastline-based coordinate system to systematically decompose TC translation into components *normal* to the coast and *alongshore*, with the aim of investigating how these components are modulated by coastline orientation and regional geographic characteristics.

This paper is organized as follows. Data and methods are described in Section 2, including a brief overview of the TC best-track data, TC selection criteria, algorithms for calculating TC translation speed and acceleration, model configuration and experimental design, and potential vorticity tendency (PVT) method. The results are presented in Section 3. Some concluding remarks and discussion are given in Section 4.

2. Data and Methods

2.1. TC Best-Track Data and Selection Criteria

The latest version of International Best Track Archive for Climate Stewardship (IBTrACS, v0401) data set is used in this study, which combines TC information from various meteorological agencies all over the world (Knapp et al., 2010). The IBTrACS includes many TC characteristics such as center location (latitude and longitude), maximum sustained wind speed (MWS), minimum central pressure, motion direction, translation speed, landfall condition, and distance to land at current location and so on. The time resolution of the data is 3 hr and the center location has a resolution of 0.1° latitude × 0.1°longitude. The landfall condition provides the minimum distance to land between the current location and the next (usually 3 hr), which can be used to identify the landfalling TCs and to determine the landfall time and location. The TC best track records for the period 1951–2023 are used in this study and 195 TCs making landfall along the South China coast are selected during this period. The selected TCs must have a peak intensity≥17.2 m/s (i.e., tropical storm intensity) and lifetimes longer than 24 hr before landfall.

2.2. Coordinate Transformation and the Decomposition of Translation Speed

To investigate the characteristics of near-landfall TCs motion in relation to the orientation of the coastline, the TC motion direction in the earth-based coordinate system is transformed into a coastline-based coordinate system

following Chan et al. (2004). Considering that the south China coast is approximately east-northeast (ENE)—west-southwest (WSW) oriented (Figure S1a in Supporting Information S1), about 72° from true-north bearing (0° in the earth-based coordinate system), the northward (southward) direction in the coastline-based coordinate system is defined as 342° (162°) and the eastward (westward) is 072° (252°) relative to the earth-based coordinate system. Based on the coastline coordinate system, a TC translation vector can be divided into normal and parallel components, which are named the TC normal-to-coast and alongshore speeds. For a TC translation speed $V(t)$ at time t, its normal-to-coast speed $V_N(t)$ and alongshore speed $V_P(t)$ components of translation speed are given as follows:

$$V_N(t) = V(t) \times \text{Cos}\,\theta(t) \tag{1}$$

$$V_P(t) = V(t) \times \text{Sin}\,\theta(t) \tag{2}$$

where the $\theta(t)$ is the angle of the TC moving direction in the coastline-based coordinate system (see Figure 1). A positive value of $V_N(t)$ means that the TC is moving toward the south China coast. Similarly, a positive value of $V_P(t)$ means that the TC is moving eastward (northeastward in the earth-based coordinate system) along the coastline. Moreover, the linear regression analysis is used to calculate the trend of TC translation speed and their changes. Statistical significance is based on the p-value of the Student's t-test.

2.3. Model Configuration and Experiment Design

Numerical simulations are carried out using the idealized TC configuration of WRF version 4.0 (Skamarock et al., 2019), with idealized TCs simulated on an f-plane under a constant Coriolis parameter of $5.0 \times 10^{-5} \text{ s}^{-1}$. The model is configured with a double-nested domain, with outer and inner domain sizes of $4,000 \times 4,000$ km and $2,000 \times 2,000$ km, respectively, and horizontal resolutions of 10 and 5 km. Double periodic boundary conditions are used in the outer inner domain. The model has 26 vertical layers and the model top is set at 25 km. Additional information on the model configuration and physical parameterization schemes used in the simulation can be found in Table S1 of Supporting Information S1.

To initialize the simulations, an axisymmetric vortex with a surface maximum tangential wind speed of 15 m s^{-1} and an RMW of 82.5 km is placed at the center of the domain, representing a weak tropical disturbance and allowing the TC to develop freely and stably from the initial conditions. For this vortex initialization, the environmental moisture, temperature profile, and wind from the Jordan sounding are used. But the sea surface temperature remains constant at 28.5°C thought the simulations.

Two experiments are conducted with the different choses of land use types. Experiment 1 (EXP1), referred to as the control experiment, has the model domain configured with a combination of rectangular sea and land surfaces. The land use types of Dryland Cropland and Pasture are 800 km west of the domain center. In contrast, Experiment 2 (EXP2) is configured with only land use types of sea surface. In both experiments, the initial vortex is embedded in a uniform easterly steering flow of 1 m s^{-1}, with $u = -1$ m s^{-1} and $v = 0$ m s^{-1}, applied throughout the entire model domain and vertical column, directing the flow toward the western side of the domain. The purpose of using a weak steering flow, rather than a strong one, is to isolate and assess the significant impact of land on changes in the translation speed of a tropical cyclone (TC), as a strong steering flow might obscure the effects of land. Additionally, the use of an easterly steering flow allows for the examination of the influence of coastline orientation on the acceleration of a landfalling TC.

2.4. Potential Vorticity Tendency (PVT) Method

The PVT method is used to diagnose the effects of land surface on changing the TC translation speed (Chan et al., 2002; Wu and Wang, 2000). The PVT equation is given as follows:

$$\left(\frac{\partial P}{\partial t}\right)_{1m} = \left(\frac{\partial P}{\partial t}\right)_{1f} + \vec{C} \cdot \nabla P_s, \tag{3}$$

where subscript 1 denotes the wavenumber-1 component of the PVT and subscripts m and f represent the moving and fixed reference frames relative to the TC center, respectively. ∇ the Hamilton operator, $\vec{C}$ the translation speed of a TC, and P_s the symmetric component of PV (P).
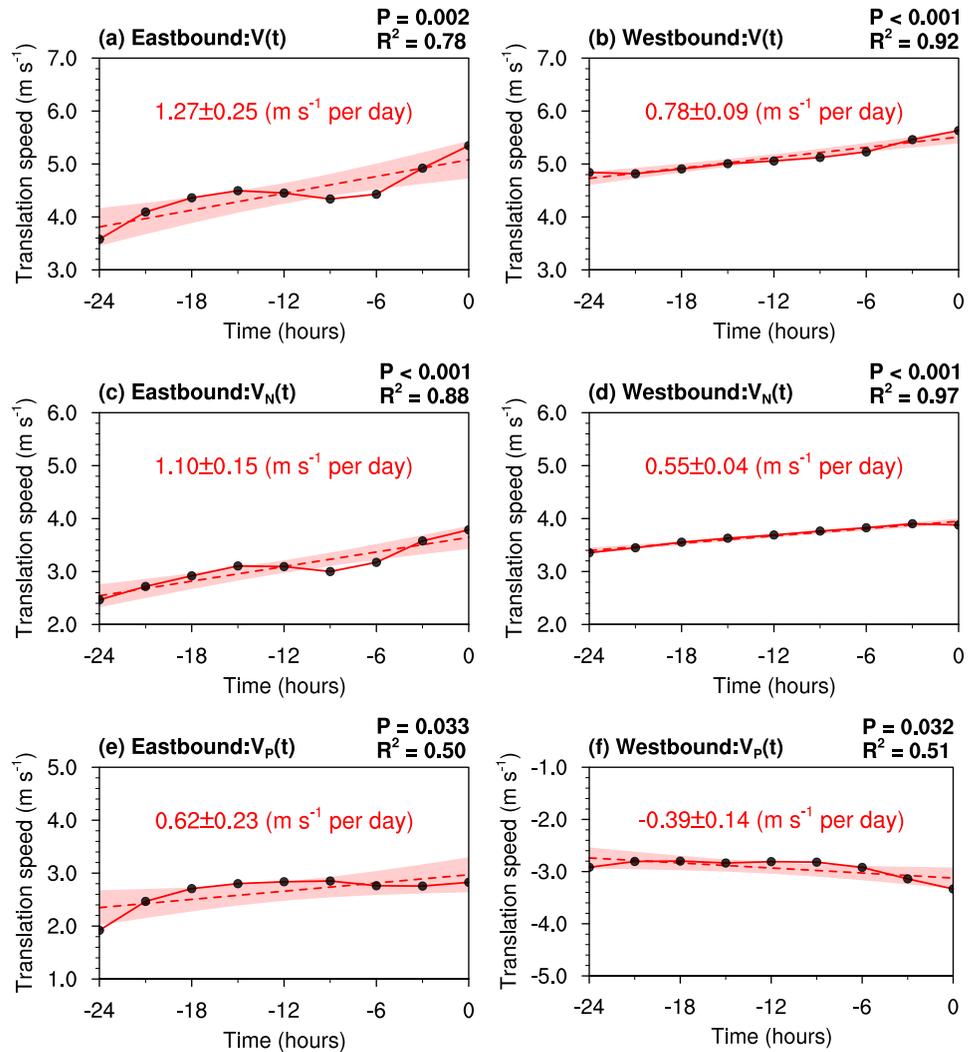
Figure 1. Time series of the mean translation speed for all landfalling TC and their linear trends. (a, b) the translation speed $V(t)$ relative to the earth-based coordinates; (c, d) the normal-to-coast $V_N(t)$ component and (e, f) the along-coast $V_P(t)$ component of translation speed relative to the coastline-based coordinate. The left and right columns represent are for eastbound and westbound TCs respectively. The red dashed lines show the linear trends of the mean translation speed. Gray shading represents the two-sided 95% confidence boundary of the linear trend. The times are presented in hours relative to landfall time (00 hr), with negative meaning hours before TC landfall. Note that the negative for the alongshore speed shown in Figure 1f means the TC are accelerating westward (southwestward in the earth-based coordinate system) along the coastline.

In the PVT equation, the PV is given as follows:

$$\left(\frac{\partial P}{\partial t}\right)_{1f} = \Lambda_1\left(-\overrightarrow{V_h}\cdot\nabla_h P - w\frac{\partial P}{\partial z} + \frac{\vec{\eta}}{\rho}\cdot\nabla\frac{d\theta_v}{dt} + R\right), \tag{4}$$

where P, $\overrightarrow{V_h}$ w and θ_v represent the potential vorticity, horizontal wind vector, vertical velocity, and virtual potential temperature, respectively. This PV equation is used to quantitatively determine the relative contributions of various physical processes to the TC translation speed, such as horizontal advection (HA), vertical advection (VA), and diabatic heating (DH). More details on the calculations of PVT and its various terms can be found in the study by Wu and Wang (2000).
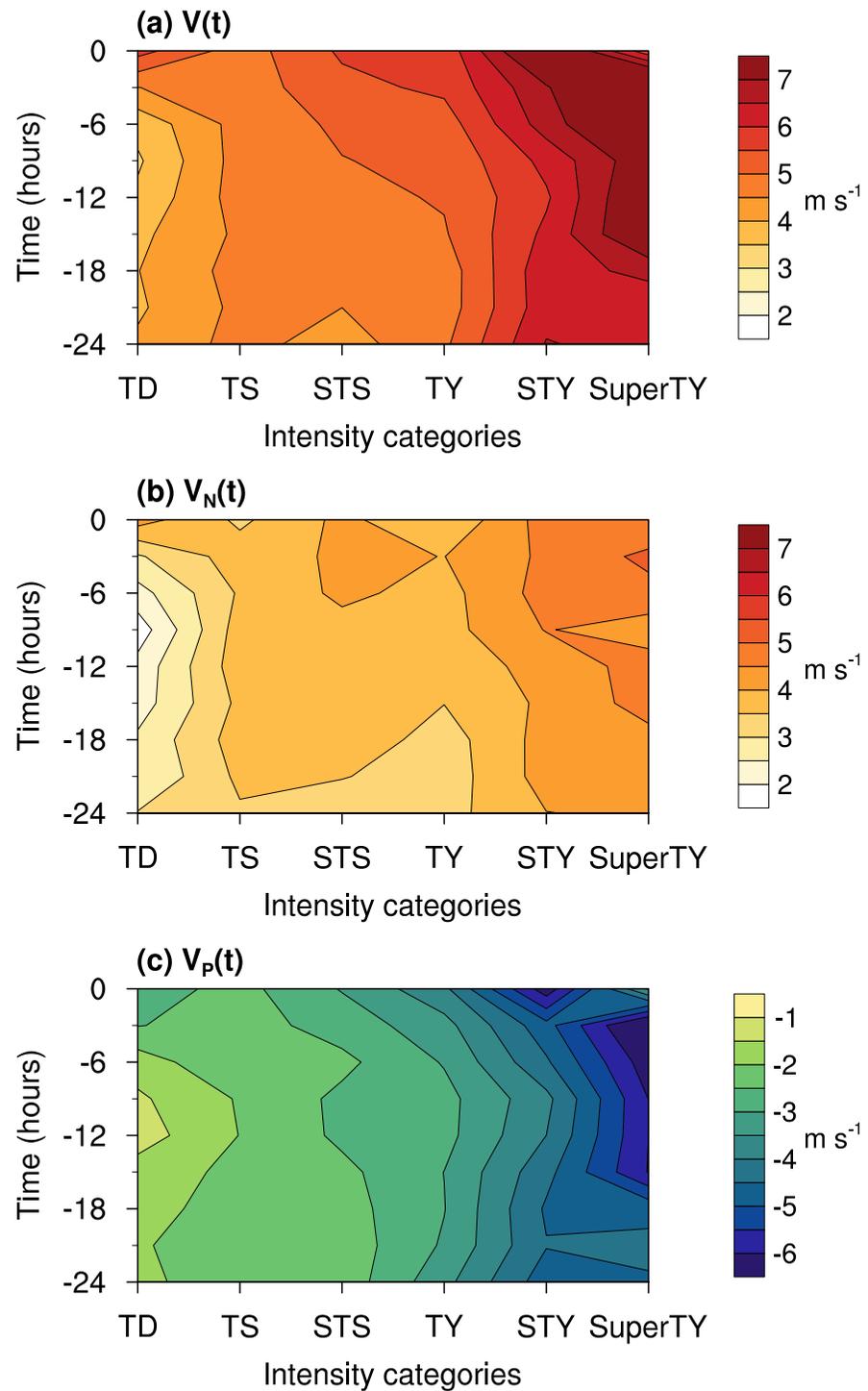
Figure 2. Changes of mean translation speed for different TC intensities for westbound TCs. (a) Translation speed in the earth coordinates; (b) the normal-to-coast and (c) along-coast components of translation speed in the coastline-based coordinates.

3. Results

3.1. Time Changes in TC Translation Speed

In order to distinguish the differences in TC motion direction, the TC tracks are first divided into eastbound and westbound paths. An eastbound (westbound) TC means that the landfall location is to the east (west) of the TC
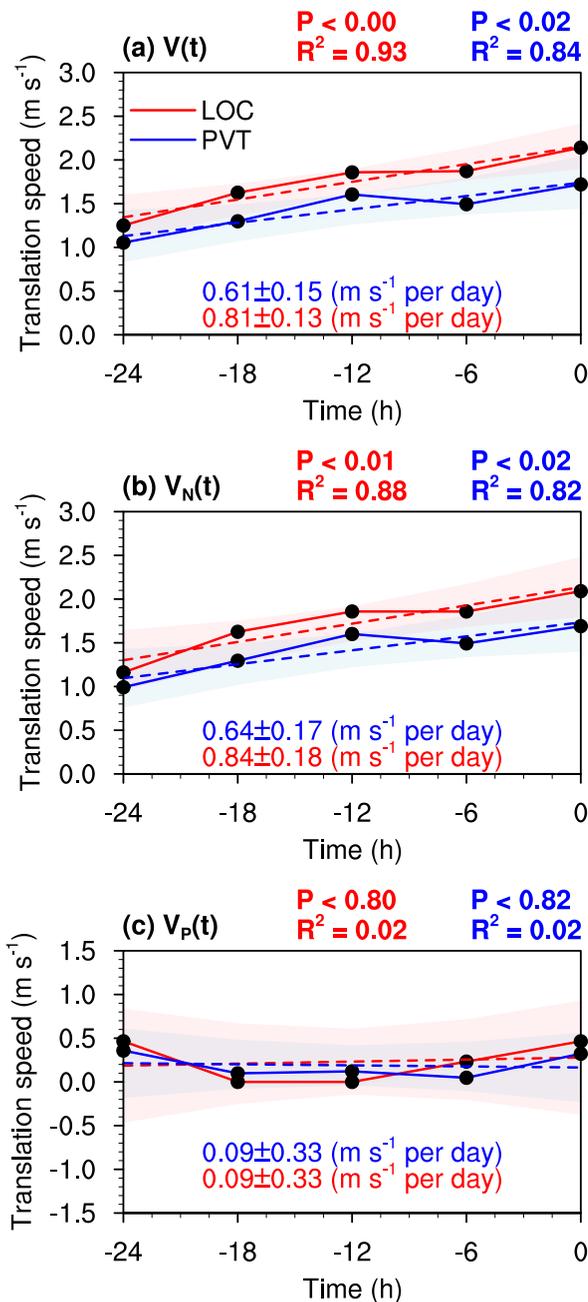
Figure 3. Time series of the translation speed for a simulated landfalling TC and their linear trends. (a) The translation speed $V(t)$ relative to the earth-based coordinates; (b) the normal-to-coast $V_N(t)$ component and (c) the along-coast $V_P(t)$ component of translation speed relative to the coastline-based coordinate. In each panel, solid blue and red lines represent potential vorticity tendency speed and location (LOC) translation speed at 6-km height, respectively. Light shading represents the two-sided 95% confidence boundary of the linear trend. Dashed lines indicate the linear regression of the translation speed with the time before landfall.

location 24 hr before it makes landfall. Figure S2 in Supporting Information S1 shows the tracks of landfalling TCs from 24 hr before making landfall to landfall time. There are 24 eastbound and 171 westbound TCs making landfall along the South China coast during 1951–2023. In other words, most of the landfalling TCs are from east to west moving close to the south China coast and then making landfall.

The time changes of the mean translation speed for the two categories of TCs show highly significant increases of TC translation speed (Figures 1a and 1b), being 35.5% and 16.4% in the 24-hr period for the eastbound and westbound TCs respectively (Table S2 in Supporting Information S1). Overall, this acceleration mainly begins around 24 hr before landfall along the South China coast, while TCs during the 72–24 hr period prior to landfall do not exhibit any acceleration (Figure S3 in Supporting Information S1).

Although acceleration is observed in both the TC normal-to-coast and alongshore speeds, the former is significantly greater than the latter (Figures 1c–1f). Specifically, the normal-to-coast speed increases by 43.0% and 16.2% in the eastbound and westbound TCs (Table S2 in Supporting Information S1), respectively, and the tendencies are similar to those of the total TC translation speed. These results indicate that landfalling TCs generally accelerate toward the coast, with the primary contribution to this acceleration arising from the normal component of their translation vector.

3.2. Relationship Between TC Translation Speed and Intensity

Previous studies have suggested that the TC translation speed may be related to its maximum wind speed, with an increase in translation speed with intensity if the TC is weaker than typhoon intensity (Mei et al., 2012; Zhang et al., 2020). However, they focused mainly on the influence of translation speed on the peak intensity of TCs over the open ocean and do not consider landfalling TCs. The changes in translation speed and acceleration for different intensity TCs are therefore further examined. Only the westbound TCs are studied because the number of eastbound TCs is too small for further classification. Our definition of TC intensity classification is similar to that in Zhang et al. (2020), but the classification is based on the current intensity. Given the current intensity of TCs varying with time, the total number for each category of TCs changes with the time. In general, the translation speed of the westbound TCs range from 2 to 7 m/s (Figure 2a), with a gradual increase in translation speed with intensity, but a relatively larger increase to >5 m/s at typhoon intensity or above. Most of this increase is in the alongshore speed (Figure 2c) and the variations in the normal-to-coast speed with intensity are relatively small (Figure 2b).

3.3. Effect of Land-Sea Contrast on the Translation Speed of a Simulated TC

To explore the underlying physics of acceleration toward the shore in landfalling TCs, we simulate two idealized TCs, both of which move toward the western side of the domain. In Experiment 1 (EXP1), the TC translation speed, that is, calculated based on the center locations, increases with statistical significance as it appr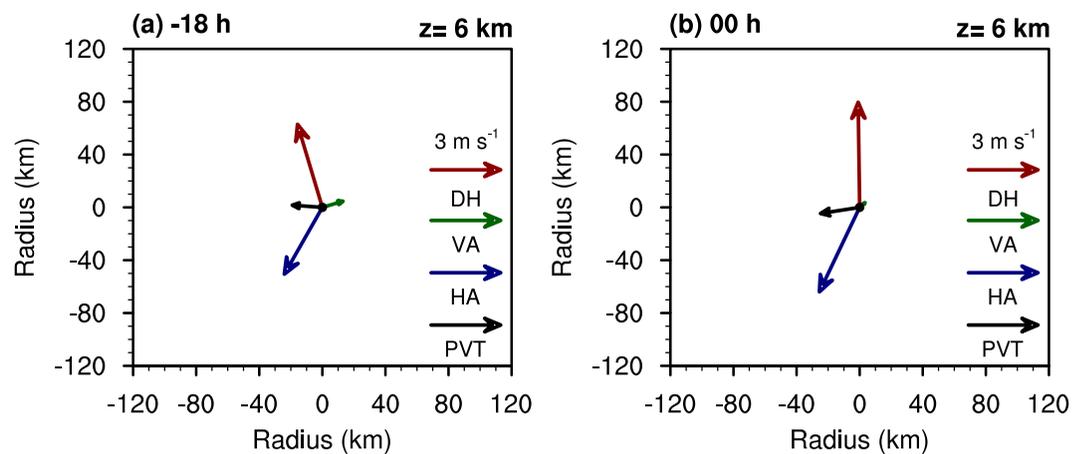oaches the coastline (Figure 3a). Specifically, this acceleration of the landfalling TC is primarily attributed to the normal component of the translation speed rather than the parallel component (Figures 3b and 3c). In contrast, Experiment 2 (EXP2) shows that no acceleration occurs as the TC moves into an area without land (Figure S4 in Supporting Information S1). These results suggest that the land effect indeed contributes to the landward acceleration of the TC as the TC approaches land.

Figure 4. Potential vorticity tendency (PVT) vector and its various components. PVT speed (black) at 6 km height and its contributions from the horizontal advection (HA, blue), vertical advection (VA, green) and diabatic heating (DH, red) terms at (a) 18 h prior to landfall (−18 hr) and (b) At the time of landfall (00 hr). The magnitude of the reference vector is 3 m s^{-1}.

Next, we further calculate the PVT translation speed and its normal and parallel components for the landfalling TCs in EXP1. The increasing trend of the PVT speed and its two components is consistent with the trend in location speed, with the main contribution to acceleration coming from the normal component of the translation speed (Figures 3a–3c). A diagnostic analysis of the PVT demonstrates that the HA and DH vectors increase as the TC approaches the coastline, both of which contribute to the increase in the normal component of PVT vector. In comparison, the contribution of VA is relatively small (Figures 4a and 4b). It is worth noting that although the individual contributions to PVT can vary with height, the retrieved PVT vectors at different levels are typically very similar. This is because the TC vortex generally maintains a vertically coherent structure, and the PVT velocity at each level represents the vector sum of contributions from the different governing processes (Wu and Wang, 2000).

These results, consistent with several studies, suggest that even in the absence of large-scale steering flows, land-induced asymmetric flow and convection can modulate the HA and DH components of PVT in a coupled manner, thereby affecting the motion of a TC near landfall (Au-Yeung and Chan, 2010; Szeto & Chan, 2010; Wong & Chan, 2006).

4. Summary and Discussion

This study not only investigates short-term changes in TC translation speed before landfall but also examines changes in the normal and parallel components of TC translation vectors relative to the orientation of the South China coast. On the average, all landfalling TCs show highly significant increases in translation speed, with the primary contribution to the total acceleration coming from the normal component of the translation vector. Based on the forward difference in translation speed, the changes in normal-to-coast accelerations for eastbound and westbound TCs are similar to those of total acceleration. Meanwhile, there is a gradual increase in translation speed of the westbound TCs with intensity, especially for typhoon intensity or above. However, the magnitude of normal-to-coast acceleration for westbound TCs does not depend on TC intensity. These results indicate that TCs, particularly as they move landward, accelerate toward the coastline 24 hr before making landfall, and the magnitude of TC landward acceleration is independent of intensity category.

In summary, although the TC motion is significantly influenced by the environmental steering flows (Chan, 2005; Chan and Gray, 1982), the physics responsible for such landward acceleration of near-landfall TCs may be not only related to the steering flows but also the land-sea contrast and boundary layer friction.

Overall, this study significantly enhances the current understanding of TC motion dynamics as it approaches the South China coast. This coastline is oriented from northeast to southwest. In fact, coastlines around the globe have highly varying orientations. For example, the west coast of North America extends from southeast to northwest, while the northeast coast follows a more north-south direction. Although the mechanism responsible for the

normal-to-coast acceleration is fundamentally universal, its impact on TC translation can be strongly modulated by the magnitude and direction of the large-scale environmental flow, which generally vary with coastal orientation. Consequently, the normal-to-coast acceleration may be partially offset or reinforced, leading to regionally different manifestations of TC acceleration or deceleration. To better understand these effects, further observational analyses using similar methods to decompose the translation speed, along with additional experiments involving different coastline orientations, are needed.

Conflict of Interest

The authors declare no conflicts of interest relevant to this study.

Data Availability Statement

The TC best-track data are obtained from the latest version of the International Best Track Archive for Climate Stewardship (IBTrACS, v0400; Knapp et al., 2010), which is available online at https://www.ncei.noaa.gov/products/international-best-track-archive.

References

Au-Yeung, A. Y., & Chan, J. C. L. (2010). The effect of a river delta and coastal roughness variation on a landfalling tropical cyclone. *Journal of Geophysical Research*, *115*(D19). https://doi.org/10.1029/2009jd013631

Chan, J. C. L. (2005). The physics of tropical cyclone motion. *Annual Review of Fluid Mechanics*, *37*(1), 99–128. https://doi.org/10.1146/annurev.fluid.37.061903.175702

Chan, J. C. L., & Gray, W. M. (1982). Tropical cyclone movement and surrounding flow relationships. *Monthly Weather Review*, *110*(10), 1354–1374. https://doi.org/10.1175/1520-0493(1982)110<1354:tcmasf>2.0.co;2

Chan, J. C. L., Ko, F. M. F., & Lei, Y. M. (2002). Relationship between potential vorticity tendency and tropical cyclone motion. *Journal of the Atmospheric Sciences*, *59*(8), 1317–1336. https://doi.org/10.1175/1520-0469(2002)059<1317:rbpvta>2.0.co;2

Chan, J. C. L., Liu, K., Ching, S. E., & Lai, E. S. (2004). Asymmetric distribution of convection associated with tropical cyclones making landfall along the South China coast. *Monthly Weather Review*, *132*(10), 2410–2420. https://doi.org/10.1175/1520-0493(2004)132<2410:adocaw>2.0.co;2

Chan, K. T. (2019). Are global tropical cyclones moving slower in a warming climate? *Environmental Research Letters*, *14*(10), 104015. https://doi.org/10.1088/1748-9326/ab4031

Emanuel, K. (2017). Assessing the present and future probability of Hurricane Harvey's rainfall. *PNAS*, *114*(48), 12681–12684. https://doi.org/10.1073/pnas.1716222114

Guo, Y.-P., Tan, Z.-M., & Chen, X. (2023). Multidecadal variability of tropical cyclone translation speed over the western North Pacific. *Journal of Climate*, *36*(17), 1–28. https://doi.org/10.1175/jcli-d-22-0760.1

Huang, P., Liang, M., Xu, J., Hu, Z., & Tu, S. (2025). Increasing variability in tropical cyclone lifetime maximum intensity over the South China Sea. *Geophysical Research Letters*, *52*(23), e2025GL119684. https://doi.org/10.1029/2025gl119684

Knapp, K. R., Kruk, M. C., Levinson, D. H., Diamond, H. J., & Neumann, C. J. (2010). The international best track archive for climate stewardship (IBTrACS) unifying tropical cyclone data [dataset]. *Bulletin America Meteorology Social*, *91*(3), 363–376. https://doi.org/10.1175/2009BAMS2755.1

Kossin, J. P. (2018). A global slowdown of tropical-cyclone translation speed. *Nature*, *558*(7708), 104–107. https://doi.org/10.1038/s41586-018-0158-3

Lanzante, J. R. (2019). Uncertainties in tropical-cyclone translation speed. *Nature*, *570*(7759), E6–E15. https://doi.org/10.1038/s41586-019-1223-2

Mei, W., Pasquero, C., & Primeau, F. (2012). The effect of translation speed upon the intensity of tropical cyclones over the tropical ocean. *Geophysical Research Letters*, *39*(7), L07801. https://doi.org/10.1029/2011gl050765

Moon, I.-J., Kim, S.-H., & Chan, J. C. L. (2019). Climate change and tropical cyclone trend. *Nature*, *570*(7759), E3–E5. https://doi.org/10.1038/s41586-019-1222-3

Risser, M. D., & Wehner, M. F. (2017). Attributable human-induced changes in the likelihood and magnitude of the observed extreme precipitation during Hurricane Harvey. *Geophysical Research Letters*, *44*(24), 12–457. https://doi.org/10.1002/2017gl075888

Sajjad, M., & Chan, J. C. L. (2019). Risk assessment for the sustainability of coastal communities: A preliminary study. *Science of the Total Environment*, *671*, 339–350. https://doi.org/10.1016/j.scitotenv.2019.03.326

Shan, K., Chu, P.-S., & Yu, X. (2023). Interdecadal change of tropical cyclone translation speed during peak season in South China Sea: Observed evidence, model results, and possible mechanism. *Journal of Climate*, *36*(13), 4531–4541. https://doi.org/10.1175/jcli-d-22-0704.1

Skamarock, W. C., & Coauthors (2019). A description of the advanced research WRF model version 4. *NCAR*, *145*, 550.

Szeto, K. C., & Chan, J. C. L. (2010). Structural changes of a tropical cyclone during landfall: Beta-plane simulations. *Advances in Atmospheric Sciences*, *27*(5), 1143–1150. https://doi.org/10.1007/s00376-009-9136-x

Wang, C., Wu, L., Lu, J., Liu, Q., Zhao, H., Tian, W., & Cao, J. (2020). Interannual variability of the basinwide translation speed of tropical cyclones in the western North Pacific. *Journal of Climate*, *33*(20), 8641–8650. https://doi.org/10.1175/jcli-d-19-0995.1

Wong, M. L. M., & Chan, J. C. L. (2006). Tropical cyclone motion in response to land surface friction. *Journal of the Atmospheric Sciences*, *63*(4), 1324–1337. https://doi.org/10.1175/jas3683.1

Wu, K., Wang, C., Wu, L., Zhao, H., & Cao, J. (2022). Slowdown in landfalling tropical cyclone motion in south China. *Geophysical Research Letters*, *49*(21), e2022GL100428. https://doi.org/10.1029/2022gl100428

Wu, L. G., & Wang, B. (2000). A potential vorticity tendency diagnostic approach for tropical cyclone motion. *Monthly Weather Review*, *128*(6), 1899–1911. https://doi.org/10.1175/1520-0493(2000)128<1899:apvtda>2.0.co;2

Yamaguchi, M., Chan, J. C., Moon, I.-J., Yoshida, K., & Mizuta, R. (2020). Global warming changes tropical cyclone translation speed. *Nature Communications*, *11*, 1–7. https://doi.org/10.1038/s41467-019-13902-y

Zhang, D., Zhang, H., Zheng, J., Cheng, X., Tian, D., & Chen, D. (2020). Changes in tropical-cyclone translation speed over the Western north Pacific. *Atmosphere*, *11*(1), 93. https://doi.org/10.3390/atmos11010093

Zhong, Q., Chan, J., Duan, W., Tu, S., Li, J., Gan, J., & Ding, R. (2025). Landfalling tropical cyclones accelerate due to land–sea thermal and roughness contrasts. *Nature Geoscience*. In Press. https://doi.org/10.1038/s41561-025-01891-1

References From the Supporting Information

Dudhia, J., & Coauthors (2008). Prediction of Atlantic tropical cyclones with the Advanced Hurricane WRF (AHW) model. In *28th conference on hurricanes and tropical meteorology, Preprints* (Vol. 18A.12). American Meteor. Society.